Supporting Information

Constructing sodiophilic interconnected ion-transport channels towards stable Na-metal anode

Yi Ding, Min Guo*, Yawei Zhang, Song Lu*, Jiadi Ying, Yeqing Wang, Tiancun Liu, Zhixin Yu*

Institute of New Energy, School of Chemistry and Chemical Engineering, Shaoxing University, Shaoxing 312000, China

Computation method

Density functional theory (DFT) calculations were performed in planewave basis set as implemented in the Vienna Ab Initio Simulation Package (VASP)[1, 2]. The exchange–correlation interactions were determined by the Perdew–Burke–Ernzerhof functional (PBE) within the generalized gradient approximation (GGA)[3]. The plane-wave basis was set with a cutoff energy of 450 eV. The convergence criteria for the energy and force was set to 1×10^{-4} eV and 0.02 eV/Å, respectively. A Monkhorst–Pack k-point mesh of 2 × 2 × 1 and 4 × 4 × 1 were used for the structure optimization and electron structure calculations, respectively. The empirical correction in Grimme's method (DFT + D3) was used to describe the van der Waals interactions. For evaluating the energy barriers, the climbing image nudged elastic band (CI-NEB) method was employed to search all transition states and pathways.[4, 5]

The binding energy (E_b) of Na^+ on different supports were calculated based on equation below:

$$E_b = E_{Na\text{-}Sub} - E_{Na} - E_{sub}$$

Where the $E_{Na\text{-}Sub}$, E_{Na}, E_{sub} are the total energies of Na-adsorbed substrate, single Na atom and clean substrate.

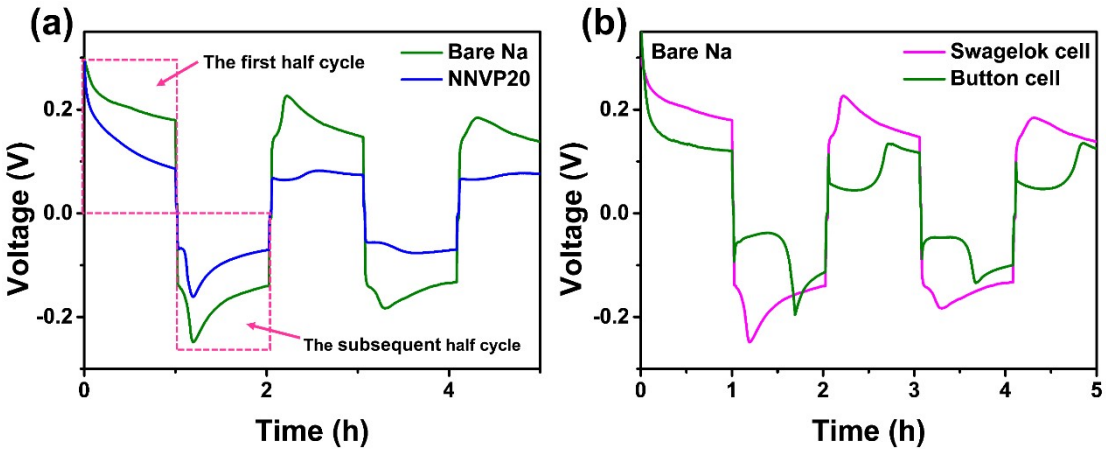

Fig S1 (a) Voltage-time curve of NNVP20||NNVP20 and Na||Na in Swagelok cell; (b) Comparison of stripping/plating curves for Na||Na cell in Swagelok cell and button cell.

Fig. S2 Photographs of bare Na foil and NNVP20 composite electrode.

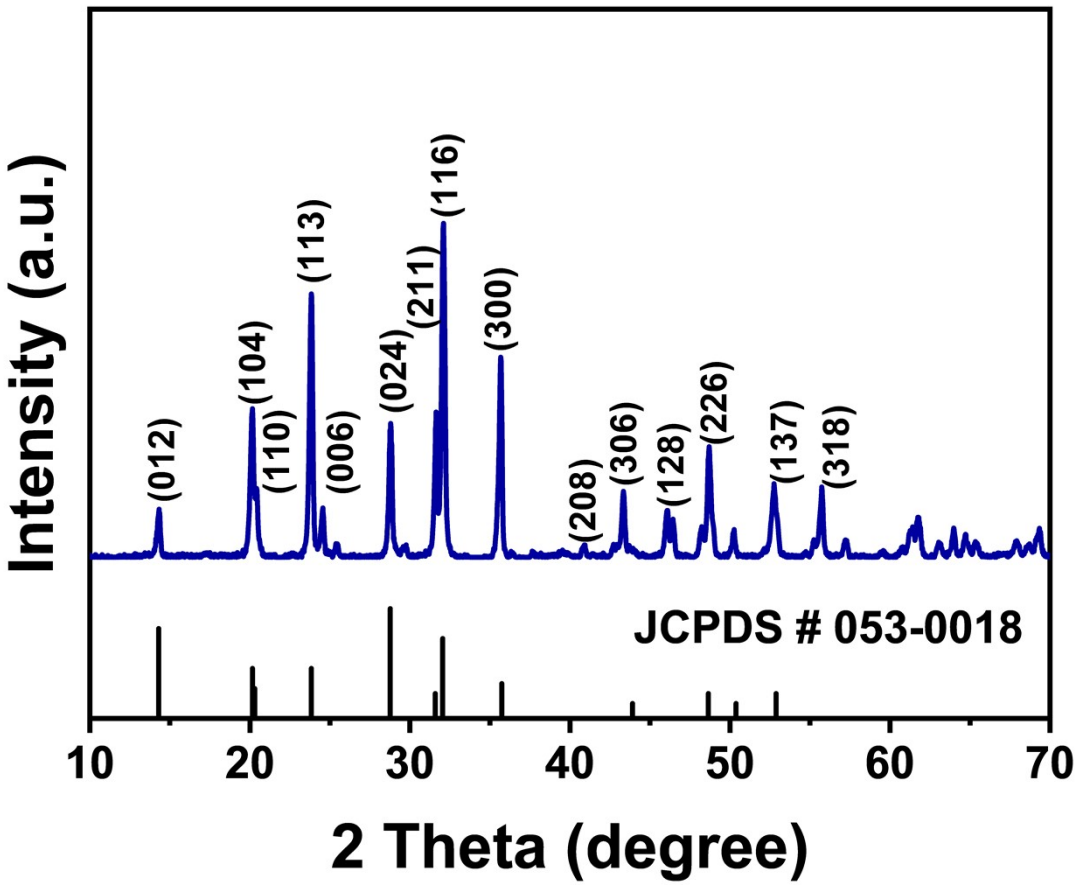

Fig. S3 X-ray diffraction spectra of NVP powder.

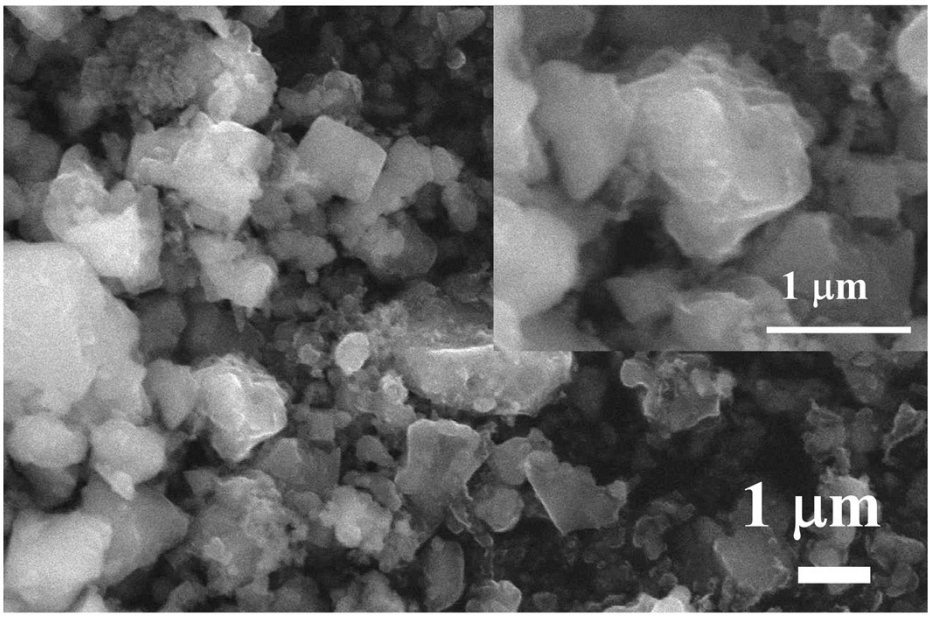

Fig. S4 SEM images of NVP.

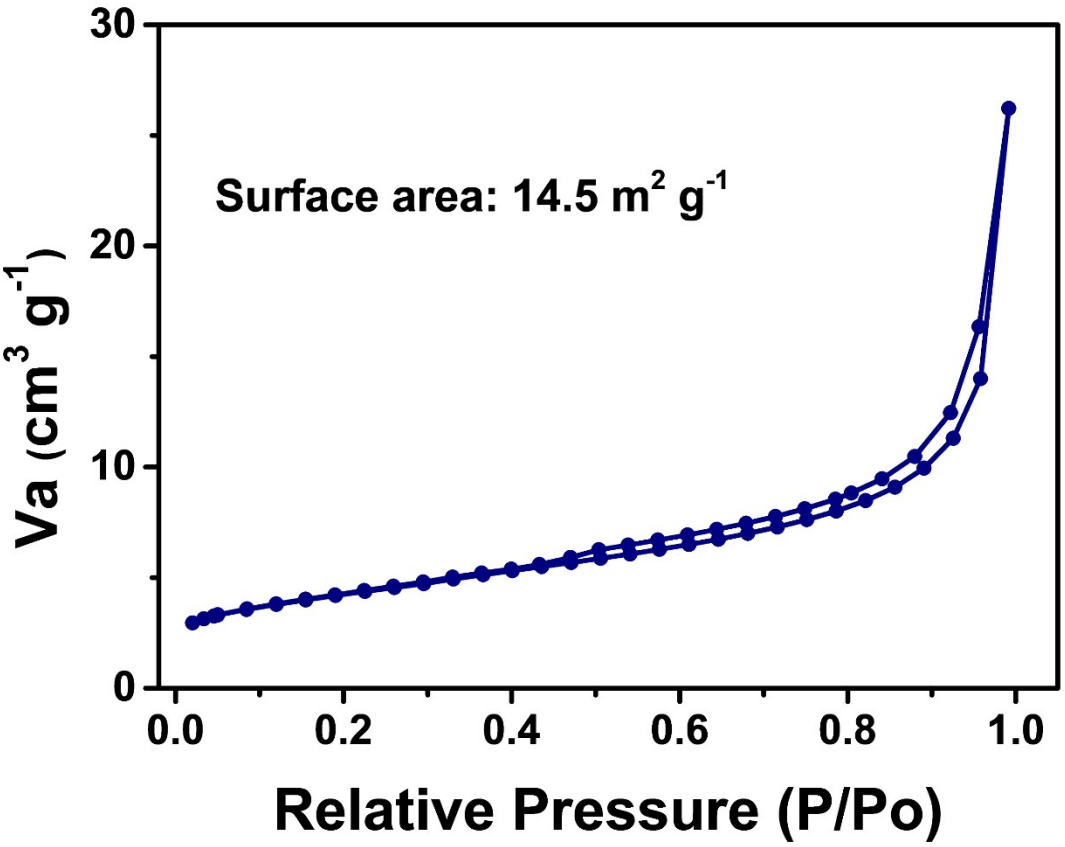

Fig. S5 Adsorption/desorption isotherms of NVP powder from N_2 physisorption.

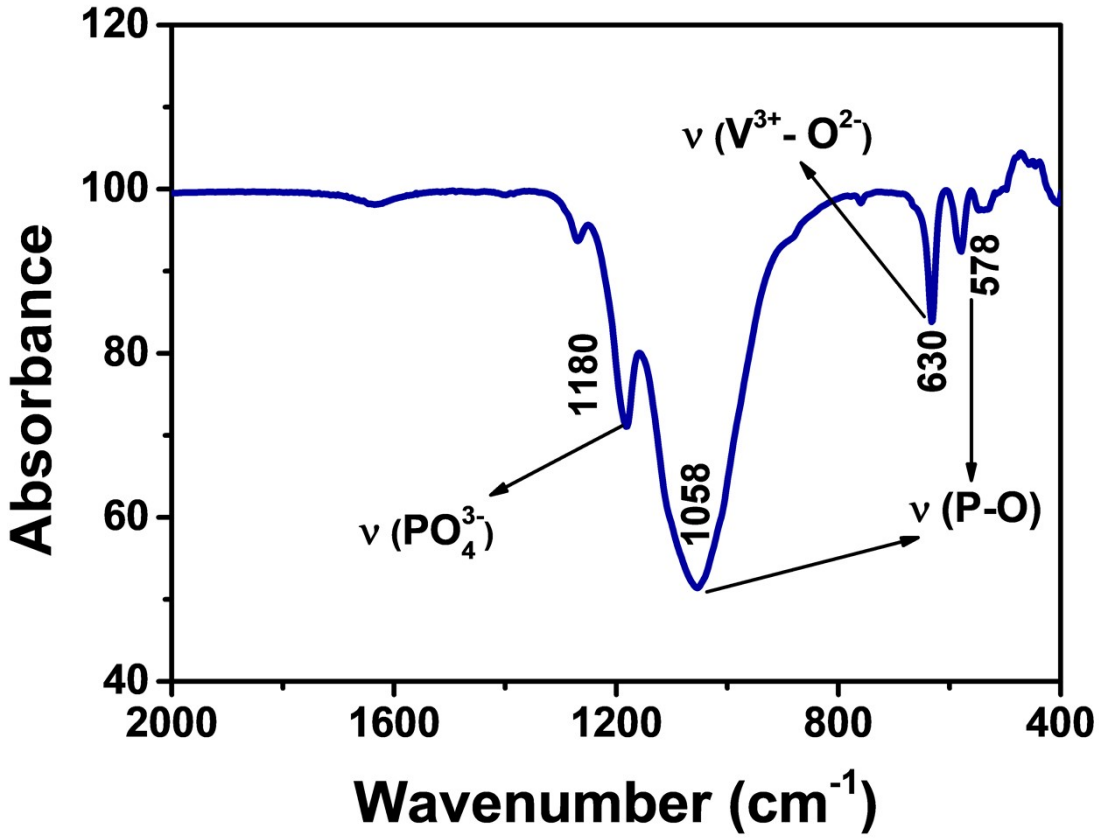

Fig. S6 FTIR spectra of NVP.

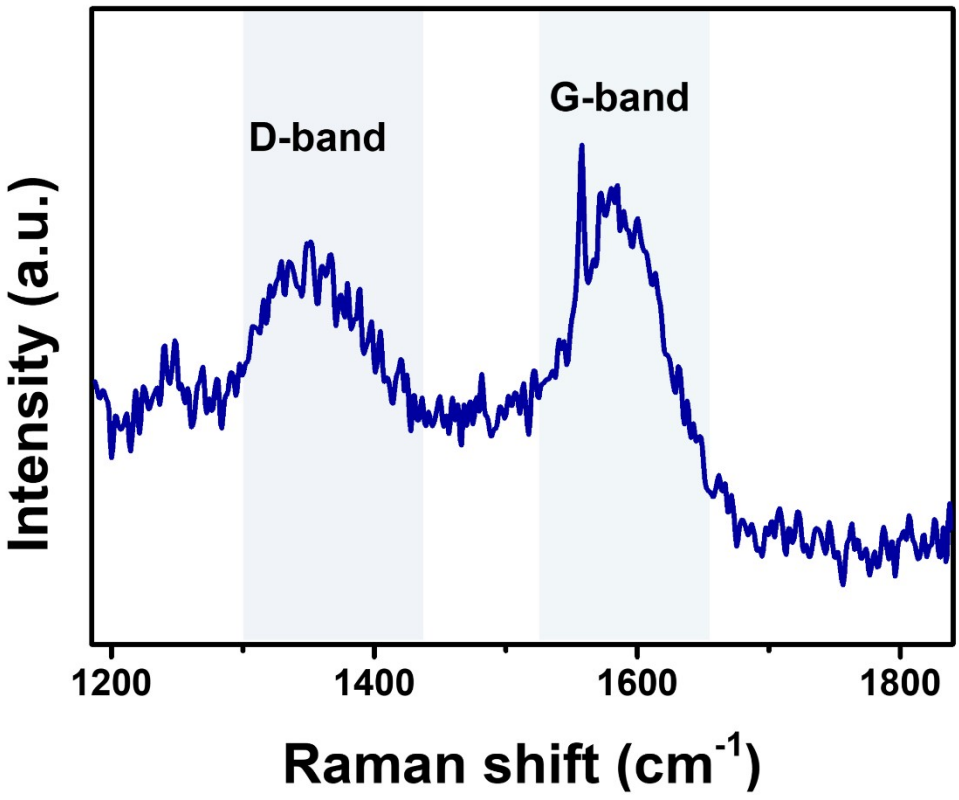

Fig. S7 Raman spectra of NVP.

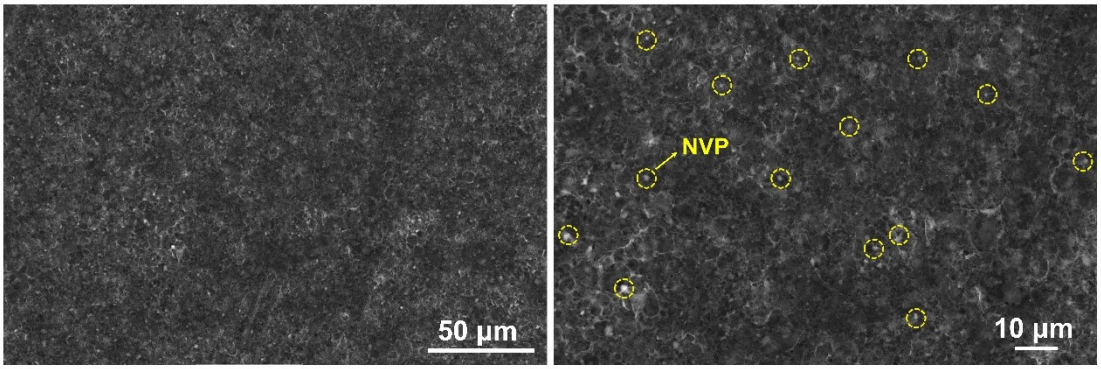

Fig. S8 Top-view SEM images of NNVP20 composite electrode.

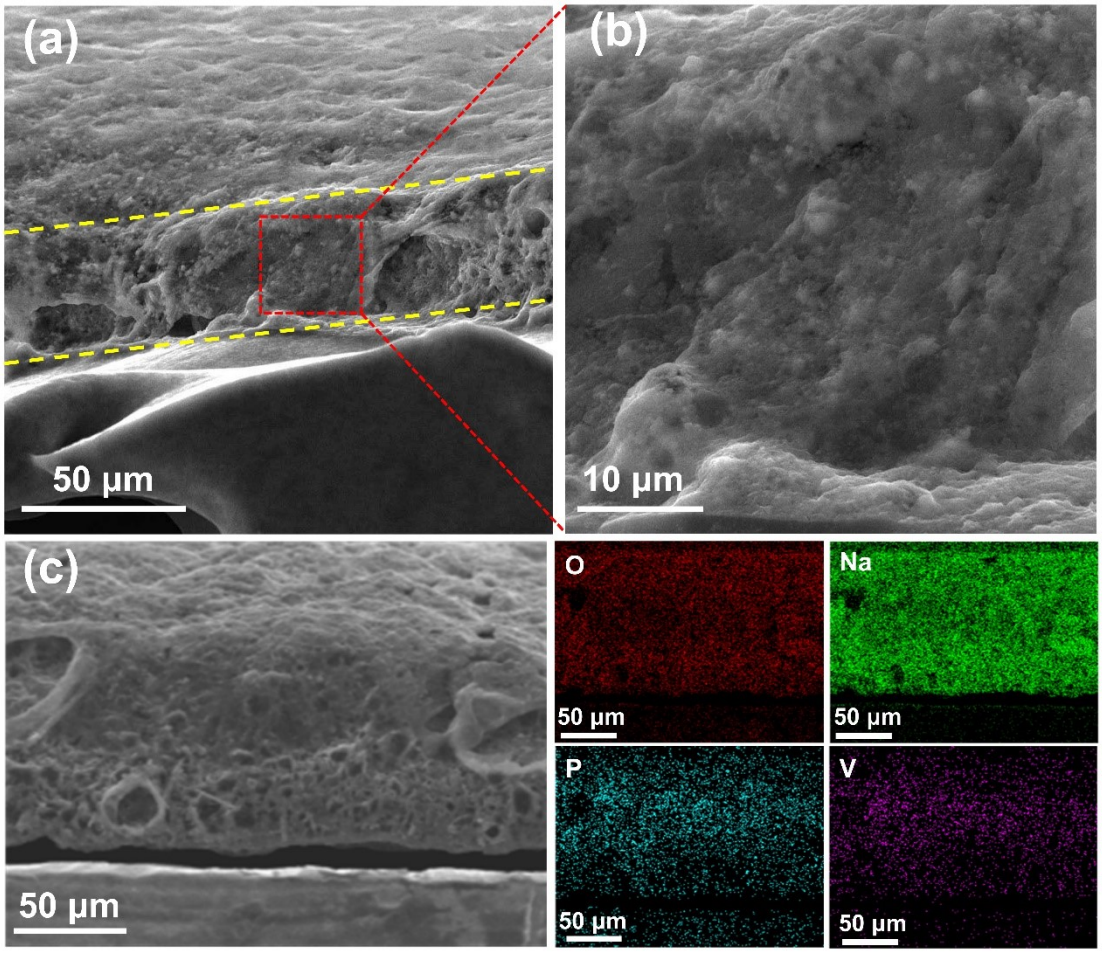

Fig S9 (a-b) Cross-sectional SEM images of NNVP20 composite electrode at different magnification, (c) EDS spectrum and elemental mappings of O, Na, P, V.

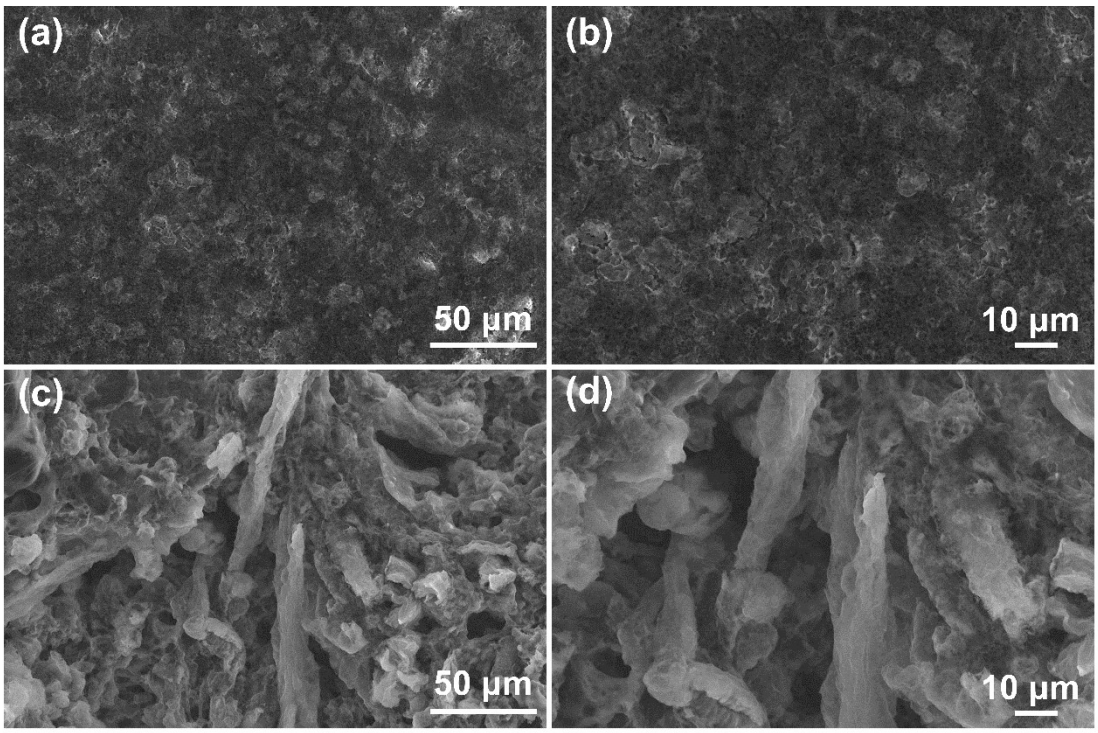

Fig S10 SEM images of bare Na electrode (a-b) before cycles, (c-d) after cycles.

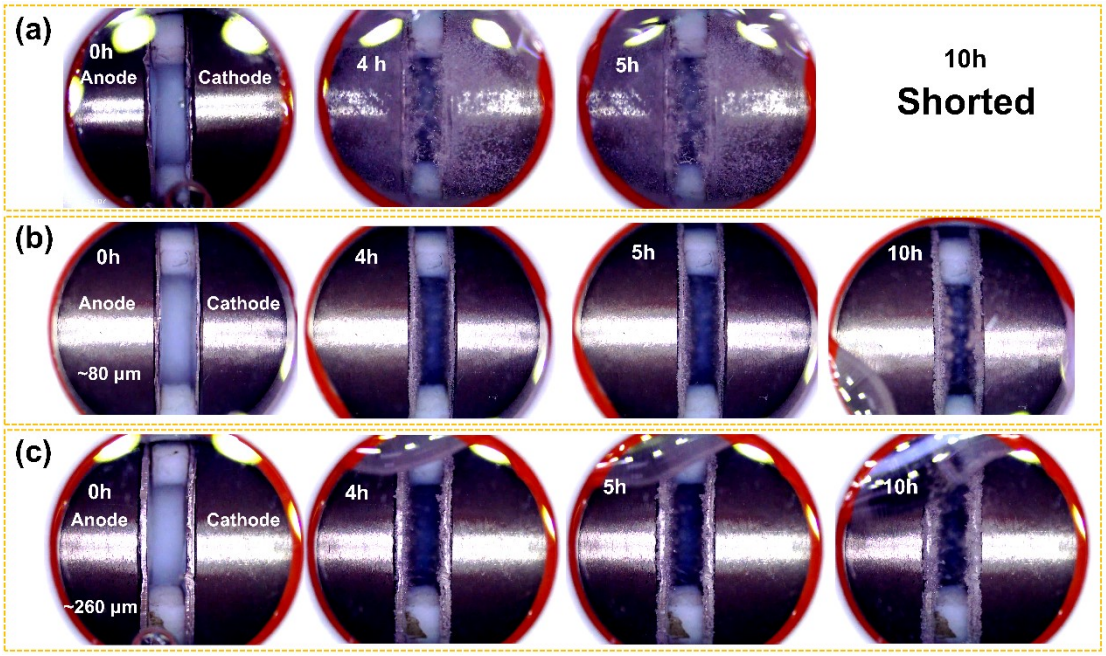

Fig S11 *In situ* optical observation of symmetric cells with different electrodes. (a) bare Na, (b) thin NNVP20 (~80 μm), (c) thick NNVP20 (~260 μm).

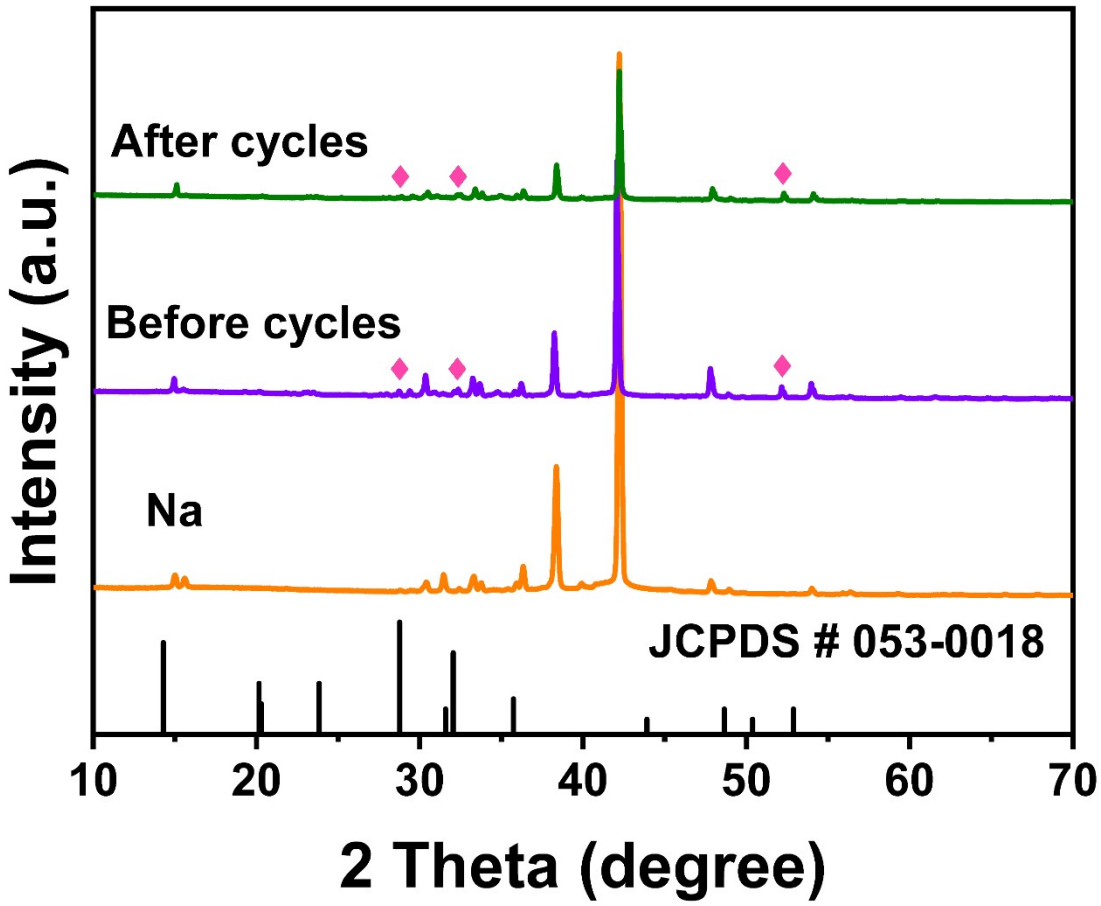

Fig S12 XRD pattern of bare Na and NNVP20 electrode before and after cycling.

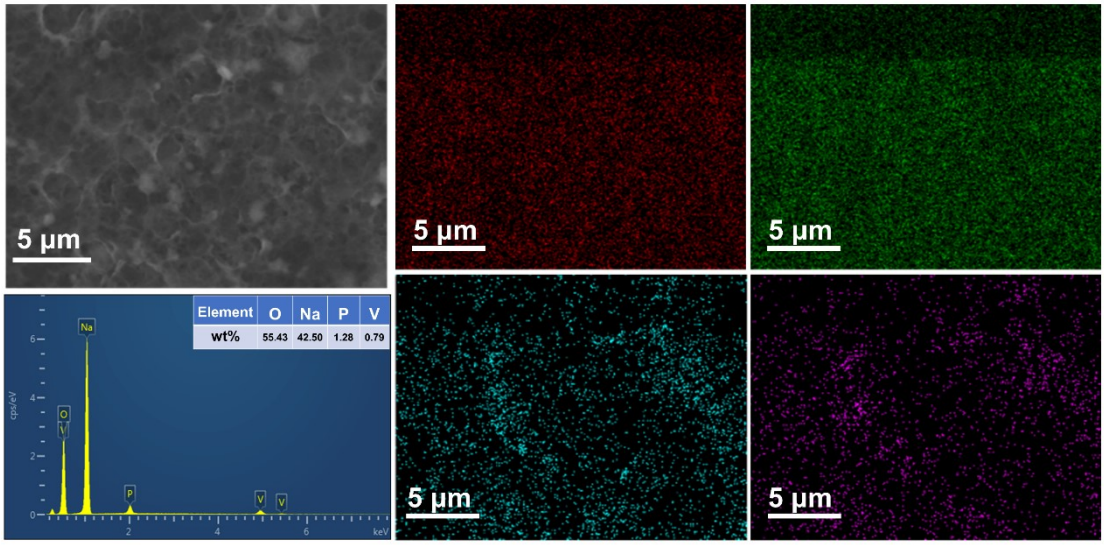

Fig S13 EDS mapping of NNVP20 electrode before cycling.

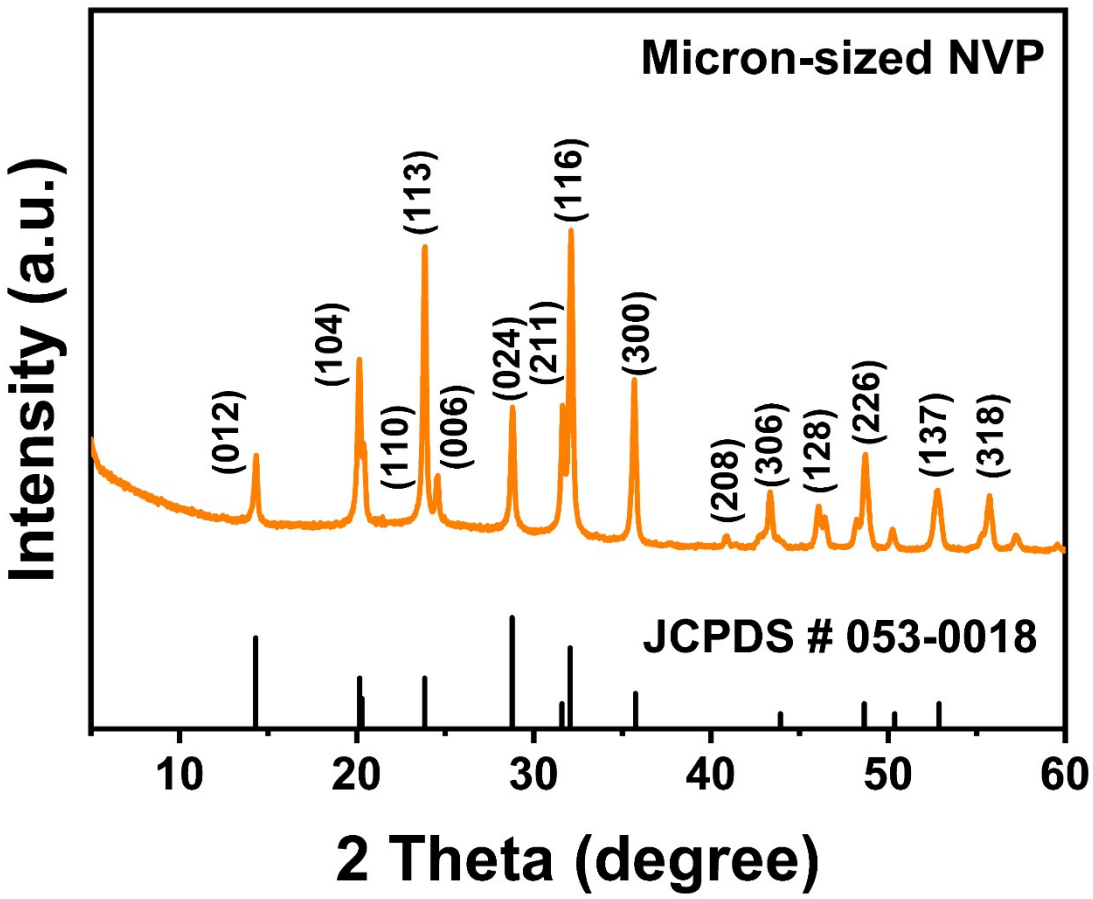

Fig S14 XRD pattern of micron-sized NVP.

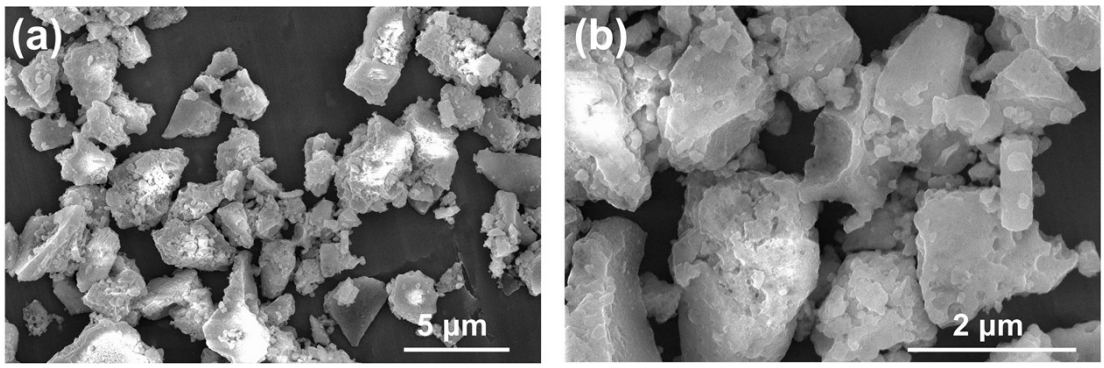

Fig S15 SEM images of micron-sized NVP.

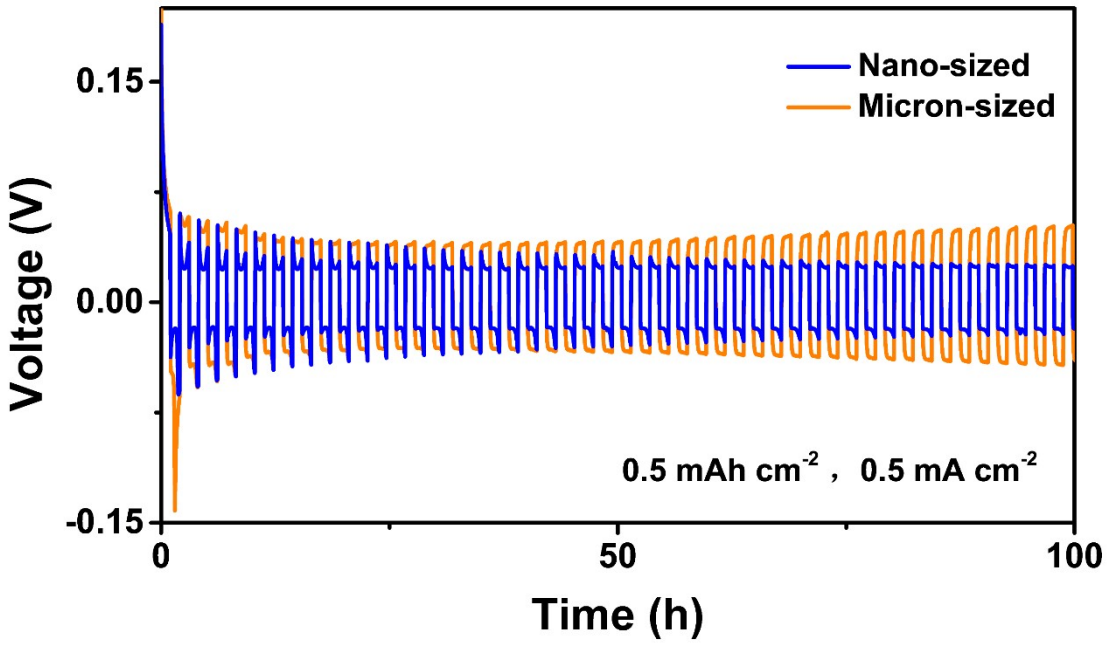

Fig S16 Voltage-time curves of micron-sized NVP-Na symmetric cell and nano-sized NVP-Na (NNVP20) electrode.

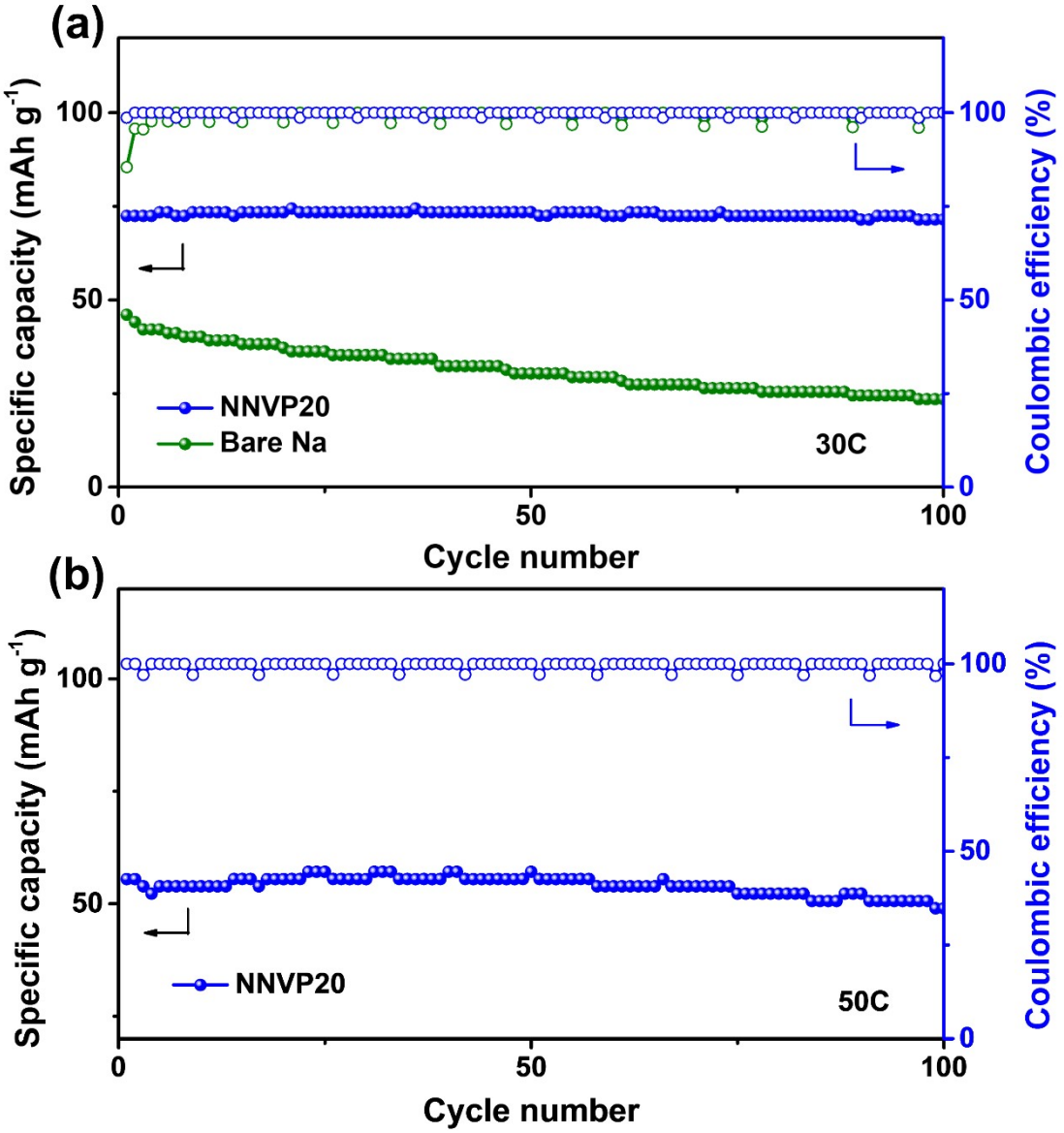

Fig S17 The cycling performances of half-cells with NVP/Na and Na anodes (a) 30C, (b) 50C.

References

1 G. Kresse and J. Furthmüller, *Phys. Rev. B*, 1996, **54**, 11169-11186.

2 G. Kresse and J. Furthmüller, *Comp. Mater. Sci.*, 1996, **6**, 15-50.

3 J. P. Perdew, K. Burke and M. Ernzerhof, *Phys. Rev. Lett.*, 1996, **77**, 3865-3868.

4 G. Henkelman, B. P. Uberuaga and H. Jónsson, *J. Chem. Phys.*, 2000, **113**, 9901-9904.

5 G. Henkelman and H. Jonsson, *J. Chem. Phys.*, 2000, **113**, 9978-9985.